



The Reading Palaeofire database: an expanded global resource to document changes in fire regimes from sedimentary charcoal records

Sandy P. Harrison^{1,2}, Roberto Villegas-Diaz¹, Esmeralda Cruz-Silva¹, Daniel Gallagher^{2,3}, David Kesner^{1,2}, Paul Lincoln^{1,2}, Yicheng Shen¹, Luke Sweeney^{1,2}, Daniele Colombaroli^{2,3}, Adam Ali⁴, Chéïma Barhoumi⁵, Yves Bergeron^{6,7}, Tatiana Blyakharchuk⁸, Přemysl Bobek⁹, Richard Bradshaw¹⁰, Jennifer L. Clear¹¹, Sambor Czerwiński¹², Anne-Laure Daniau¹³, John Dodson^{14,15}, Kevin J. Edwards^{16,17}, Mary E. Edwards¹⁸, Angelica Feurdean¹⁹, David Foster²⁰, Konrad Gajewski²¹, Mariusz Gałka²², Michelle Garneau²³, Thomas Giesecke²⁴, Graciela Gil Romera^{25,26}, Martin P. Girardin²⁷, Dana Hoefler²⁸, Kangyou Huang²⁹, Jun Inoue³⁰, Eva Jamrichová⁹, Nauris Jasiunas³¹, Wenying Jiang³², Gonzalo Jiménez-Moreno³³, Monika Karpińska-Kołaczek¹², Piotr Kołaczek¹², Niina Kuosmanen³⁴, Mariusz Lamentowicz³⁵, Martin Lavoie³⁶, Fang Li³⁷, Jianyong Li³⁸, Olga Lisitsyna^{39,40}, José Antonio López-Sáez⁴¹, Reyes Luelmo-Lautenschlaeger⁴¹, Gabriel Magnan²³, Eniko Katalin Magyari⁴², Alekss Maksims⁴³, Katarzyna Marcisz¹², Elena Marinova⁴⁴, Jenn Marlon⁴⁵, Scott Mensing⁴⁶, Joanna Mirosław-Grabowska⁴⁷, Wyatt Oswald^{20,48}, Sebastián Pérez-Díaz⁴⁹, Ramón Pérez-Obiol⁵⁰, Sanna Piilo⁵¹, Anneli Poska^{39,52}, Xiaoguang Qin⁵³, Cécile C. Remy⁵⁴, Pierre Richard⁵⁵, Sakari Salonen³⁴, Naoko Sasaki⁵⁶, Hieke Schneider⁵⁷, William Shotyk⁵⁸, Migle Stancikaite⁵⁹, Dace Šteinberga⁴³, Normunds Stivrins^{31,39,60}, Hikaru Takahara⁶¹, Zhihai Tan⁶², Liva Trasune^{31,34}, Charles E. Umbanhowar⁶³, Minna Väiliranta⁵¹, Jüri Vassiljev³⁹, Xiayun Xiao⁶⁴, Qinghai Xu⁶⁵, Xin Xu³⁷, Edyta Zawisza⁶⁶, Yan Zhao⁶⁷, Zheng Zhou²⁹

- 1: School of Archaeology, Geography & Environmental Science, Reading University, Whiteknights, Reading, RG6 6AH, UK
- 2: Leverhulme Centre for Wildfires, Environment and Society, Imperial College London, South Kensington, London, SW7 2BW, UK
- 3: Department of Geography, Royal Holloway, University of London, Egham, TW20 0 SS, UK
- 4: University de Montpellier, Institut des Sciences de l'Evolution (CNRS, IRD, EPHE), France
- 5: Department of Palynology and Climate Dynamics, Albrecht-von-Haller Institute for Plant Sciences, University of Göttingen, Untere Karspüle 2, 37073 Göttingen, Germany
- 6: Forest Research Institute (IRF), Université du Québec en Abitibi-Témiscamingue (UQAT), Rouyn-Noranda, QC, Canada J9X 5E4
- 7: Department of Biological Sciences, Université du Québec à Montréal (UQAM), Montréal, QC, Canada H3C 3P8
- 8: Institute of Monitoring of Climatic and Ecological Systems of Siberian branch of Russian Academy of Sciences (IMCES SB RAS), Tomsk, 634055, Russia
- 9: Institute of Botany, Czech Academy of Sciences, Lidická 25/27, 602 00 Brno, Czech Republic



- 10: Geography and Planning, University of Liverpool, Liverpool, L69 7ZT, UK
- 11: Department of Geography and Environmental Science, Liverpool Hope University, Taggart Street, Childwall, Liverpool, L16 9JD, UK
- 12: Climate Change Ecology Research Unit, Faculty of Geographical and Geological Sciences, Adam Mickiewicz University, Poznań, Bogumiła Krygowskiego 10, 61-680 Poznań, Poland
- 13: Environnements et Paléoenvironnements Océaniques et Continentaux (EPOC), Unité Mixte de Recherche (UMR) 5805, Centre National de la Recherche Scientifique (CNRS), Université de Bordeaux, 33615 Pessac, France
- 14: Institute of Earth Environment, Chinese Academy of Sciences, Keji 1st Rd, Yanta District, Xi'an, Shaanxi, China
- 15: School of Earth, Atmospheric and Life Sciences, University of Wollongong, Wollongong, NSW 2500, Australia
- 16: Department of Geography & Environment and Archaeology, University of Aberdeen, Aberdeen AB24 3UX, UK
- 17: McDonald Institute for Archaeological Research and Scott Polar Research Institute, University of Cambridge, Cambridge, UK
- 18: School of Geography and Environmental Science, University of Southampton, Southampton SO17 1BJ, UK
- 19: Department of Physical Geography, Goethe University, Altenhöferallee 1, 60438 Frankfurt am Main, Germany
- 20: Harvard Forest, Harvard University, Petersham MA 01366 USA
- 21: Département de Géographie, Environnement et Géomatique, Université d'Ottawa, Ottawa, ON, K1N6N5 Canada
- 22: University of Lodz, Faculty of Biology and Environmental Protection, Department of Biogeography, Paleoecology and Nature Protection, 1/3 Banacha Str., 90-237 Lodz, Poland
- 23: GEOTOP Research Center, Université du Québec à Montréal, Montréal QC, H2X 3Y7, Canada
- 24: Department of Physical Geography, Faculty of Geosciences, Utrecht University, Netherlands
- 25: Instituto Pirenaico de Ecología-CSIC, Avda. Montañana 1005, 50059, Zaragoza, Spain
- 26: Plant Ecology & Geobotany, Karl-Von-Frisch-Straße 8, Philipps University of Marburg, Marburg
- 27: Natural Resources Canada, Canadian Forest Service, Laurentian Forestry Centre, Quebec City, QC, Canada
- 28: Senckenberg Research Station of Quaternary Palaeontology, Am Jakobskirchhof 4, 99423 Weimar, Germany
- 29: School of Earth Sciences and Engineering, Sun Yat-sen University, Zhuhai 519082, China
- 30: Department of Geosciences, Graduate School of Science, Osaka City University, Osaka, Japan
- 31: Department of Geography, University of Latvia, Jelgavas iela 1, Riga, LV-1004, Latvia
- 32: Key Laboratory of Cenozoic Geology and Environment, Institute of Geology and Geophysics, Chinese Academy of Sciences, Beijing, China
- 33: Departamento de Estratigrafía y Paleontología, Facultad de Ciencias, Universidad de Granada, Avda. Fuente Nueva S/N, 18002 Granada, Spain
- 34: Department of Geosciences and Geography, University of Helsinki, P.O.Box 64, FI-00014, Helsinki, Finland
- 35: Faculty of Geographical and Geological Sciences, Adam Mickiewicz University in Poznan, Bogumiła Krygowskiego 10, 61-680 Poznan, Poland



- 36: Département de géographie, Université Laval, Québec, Canada
- 37: International Center for Climate and Environment Sciences, Institute of Atmospheric Physics, Chinese Academy of Sciences, Beijing, China
- 38: Shaanxi Key Laboratory of Earth Surface System and Environmental Carrying Capacity, College of Urban and Environmental Sciences, Northwest University, Xi'an 710127, China
- 39: Department of Geology, Tallinn University of Technology, Ehitajate tee 5, 19086 Tallinn, Estonia
- 40: Russian State Agrarian University, Timiryazevskaya st., 49, 127550, Moscow, Russia
- 41: Environmental Archaeology Research Group, Institute of History, CSIC, Madrid, Spain
- 42: Department of Environmental and Landscape Geography, ELKH-MTM-ELTE Research Group for Paleontology, Eotvos Lorand university, 1117 Budapest, Pazmany Peter stny 1/c, Budapest, Hungary
- 43: Department of Geology, University of Latvia, Jelgavas iela 1, Riga, LV-1004, Latvia
- 44: Laboratory for Archaeobotany, State Office for Cultural Heritage Baden-Württemberg, Fischersteig 9, 78343 Geienhofen-Hemmenhofen, Germany
- 45: Yale School of the Environment, New Haven, Connecticut 06511, USA
- 46: Department of Geography, University of Nevada Reno, 1664 N Virginia St, Reno, NV 89557, USA
- 47: Institute of Geological Sciences, Polish Academy of Sciences, Warsaw, Poland
- 48: Marlboro Institute for Liberal Arts and Interdisciplinary Studies, Emerson College, Boston MA 02116 USA
- 49: Department of Geography, Urban and Regional Planning, University of Cantabria, Santander, Spain
- 50: Unitat de Botànica, Facultat de Biociències, Universitat Autònoma de Barcelona, Cerdanyola del Vallès, 08193 Barcelona, Spain
- 51: Environmental Change Research Unit (ECRU), Ecosystems, Environment Research Programme, Faculty of Biological and Environmental Sciences, Viikinkaari 1, P.O. Box 65, 00014 University of Helsinki, Finland
- 52: Department of Physical Geography and Ecosystem Science, Lund University, Lund, Sweden
- 53: Key Laboratory of Cenozoic Geology and Environment, Institute of Geology and Geophysics, Chinese Academy of Sciences, No.19 Beitucheng West RD, Beijing, 100029, China
- 54: Institut für Geographie, Universität Augsburg, 86135 Augsburg, Germany
- 55: Département de géographie, Complexe des sciences, Université de Montréal, Montréal, H2V 0B3, Canada
- 56: Graduate School of Life and Environmental Sciences, Kyoto Prefectural University, 1-5 Hangi-cho, Shimogamo, Sakyo-ku, Kyoto 606-8522, Japan
- 57: Institut für Geographie, Friedrich-Schiller-Universität Jena, Löbdergraben 32, 07743 Jena, Germany
- 58: Department of Renewable Resources, University of Alberta, 348B South Academic Building, Edmonton, Alberta T6G 2H1, Canada
- 59: Institute of Geology and Geography, Nature Research Centre, Akademijos Str. 2, LT-08412, Vilnius, Lithuania
- 60: Latvian Institute of History, University of Latvia, Kalpaka blv. 4, Riga, LV-1050, Latvia
- 61: Graduate School of Agriculture, Kyoto Prefectural University, Shimogamo, Sakyo-ku, 1-5, Hangi-cho, 606-8522 Kyoto, Japan
- 62: School of Environment and Chemistry Engineering, Xi'an Polytechnic University, Xi'an, Shaanxi 710048, China



63: Departments of Biology and Environmental Studies, St Olaf College, 1520 St Olaf Ave,
Northfield, MN 55057, USA

64: State Key Laboratory of Lake Science and Environment, Nanjing Institute of Geography
and Limnology, Chinese Academy of Sciences, Nanjing 210008, China

65: College of Resources and Environment Sciences, Hebei Normal University, Shijiazhuang
050024, China

66: Institute of Geological Sciences, Polish Academy of Sciences, Twarda 51/55, 00-818 Warsaw,
Poland

67: Institute of Geographic Sciences and Natural Resources Research, Chinese Academy of
Sciences, Beijing 100101, China

Corresponding author: Sandy P. Harrison, s.p.harrison@reading.ac.uk



1 **Abstract**

2 Sedimentary charcoal records are widely used to reconstruct regional changes in fire regimes
3 through time in the geological past. Existing global compilations are not geographically
4 comprehensive and do not provide consistent metadata for all sites. Furthermore, the age
5 models provided for these records are not harmonised and many are based on older calibrations
6 of the radiocarbon ages. These issues limit the use of existing compilations for research into
7 past fire regimes. Here, we present an expanded database of charcoal records, accompanied by
8 new age models based on recalibration of radiocarbon ages using INTCAL2020 and Bayesian
9 age-modelling software. We document the structure and contents of the database, the
10 construction of the age models, and the quality control measures applied. We also record the
11 expansion of geographical coverage relative to previous charcoal compilations and the
12 expansion of metadata that can be used to inform analyses. This first version of the Reading
13 Palaeofire Database contains 1681 records (entities) from 1477 sites worldwide. The database
14 (DOI: 10.17864/1947.319) is available from <https://researchdata.reading.ac.uk/id/eprint/319>.



15 **1. Introduction**

16

17 Wildfires have major impacts on terrestrial ecosystems (Bond et al., 2005; Bowman et al.,
18 2016; He et al., 2019; Lasslop et al., 2020), the global carbon cycle (Li et al., 2014; Arora and
19 Melton, 2018; Pellegrini et al., 2018; Lasslop et al., 2019), atmospheric chemistry (van der
20 Werf et al., 2010; Voulgarakis and Field, 2015; Sokolik et al., 2019) and climate (Randerson
21 et al., 2006; Li et al., 2017; Harrison et al., 2018; Liu et al., 2019). Although the climatic,
22 vegetation and anthropogenic controls on wildfires are relatively well understood (e.g.
23 Harrison et al., 2010; Bistinas et al., 2014; Knorr et al., 2016; Forkel et al., 2017; Li et al.,
24 2019), recent years have seen wildfires occurring in regions where they were historically rare
25 (e.g. northern Alaska, Greenland, northern Scandinavia) and an increase in fire frequency and
26 severity in more fire-prone regions (e.g. California, the circum-Mediterranean, eastern
27 Australia). It is useful to look at the pre-industrial era (conventionally defined as pre 1850 CE)
28 to understand whether these events are atypical. The pre-industrial past also provides an
29 opportunity to characterise fire regimes before anthropogenic influences, both in terms of
30 ignitions and fire suppression, became important.

31

32 Ice-core records provide a global picture of changes in wildfire in the geologic past (Rubino et
33 al., 2016). However, wildfires exhibit considerable local to regional variability because of the
34 spatial heterogeneity of the various factors controlling their occurrence and intensity. Thus, it
35 is useful to use information that can provide a picture of regional changes through time.
36 Charcoal, preserved in lake, peat or marine sediments, can provide a picture of such changes.
37 The wildfire regime can be characterised from sedimentary charcoal records through total
38 charcoal abundance per unit of sediment, which can be considered as a measure of the total
39 biomass burned (e.g. Marlon et al., 2006) or by the presence of peaks in charcoal accumulation
40 which, in records with sufficiently high temporal resolution, can indicate individual episodes
41 of fire (e.g. Power et al., 2006).

42

43 The Global Palaeofire Working Group (GPWG) was established in 2006 to coordinate the
44 compilation and analysis of charcoal data globally, through the construction of the Global
45 Charcoal Database (GCD: Power et al., 2008). The GPWG was initiated by the International
46 Geosphere-Biosphere Programme (IGBP) Fast-Track Initiative on Fire and subsequently
47 recognised as a working group of the Past Global Changes (PAGES) Project in 2008. There
48 have now been several iterations of the GCD (Power et al., 2008; Power et al., 2010; Daniau



49 et al., 2012; Blarquez et al., 2014; Marlon et al., 2016), which since 2020 has been managed
50 by the International Palaeofire Network as the Global Palaeofire Database (GPD;
51 <https://paleofire.org>). The GCD has been used to examine changes in fire regimes over the past
52 two millennia (Marlon et al., 2008), during the current interglacial (Marlon et al., 2013), on
53 glacial-interglacial timescales (Power et al., 2008; Danialu et al., 2012; Williams et al., 2015)
54 and in response to rapid climate changes (Marlon et al., 2009; Danialu et al., 2010), as well as
55 to examine regional fire histories (e.g. Mooney et al., 2011; Vanni re et al., 2011; Marlon et
56 al., 2012; Power et al., 2013; Feurdean et al., 2020). However, there are a number of limitations
57 to the use of the GCD for analyses of palaeofire regimes. Firstly, the database does not include
58 many recently published records and needs to be updated. Secondly, there are inconsistencies
59 among the various versions of the database including duplicated and/or missing sites,
60 differences in the metadata included for each site or record, and missing metadata for some
61 sites or records. Perhaps most crucially, the age models included in the database were made at
62 different times, using different radiocarbon calibration curves, and using different age-
63 modelling methods. The disparities between the archived age models preclude a detailed
64 comparison of changes in wildfire regimes across regions.

65

66 Here, we present an expanded database of charcoal records (the Reading Palaeofire Database,
67 RPD), accompanied by new age models based on recalibration of radiocarbon ages using
68 INTCAL2020 (Reimer et al., 2020) and using a consistent Bayesian approach (BACON:
69 Blaauw et al., 2021) to age-model construction. We document the structure and contents of
70 the database, the construction of the new age models, the expanded metadata available, and the
71 quality control measures applied to check the data entry. We also document the expansion of
72 the geographic and temporal coverage, and in the availability of metadata, relative to previous
73 GCD compilations.

74

75

76 **2. Data and Methods**

77

78 ***2.1. Compilation of data***

79

80 The database contains sedimentary charcoal records, metadata to facilitate the interpretation of
81 these records, and information on the dates used to construct the original age model for each
82 record. Some records were obtained from the GCD. There are multiple versions of the GCD

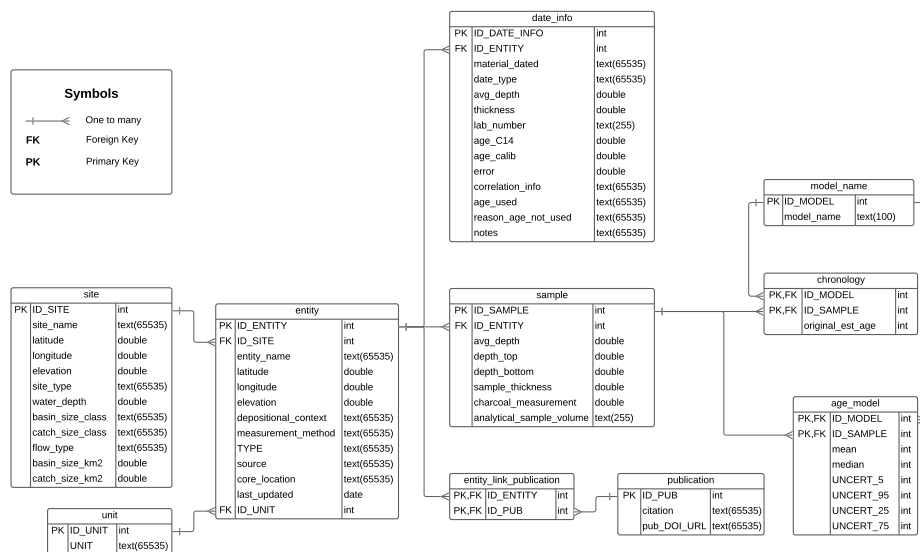


83 which differ in terms of the sites and the types of metadata included. We compared the GCDv3
84 (Marlon et al., 2016), GCDv4 (Blarquez, 2018) and GCD webpage versions
85 (<http://paleofire.org>) and extracted a single unique version of each site and entity across the
86 three versions. Where sites or entities were duplicated in different versions of the GCD, we
87 used the latest version. Missing metadata and dating information for these records were
88 obtained from the literature or from the original data providers. Some sites in the GCD were
89 represented by both concentration data and the same data expressed as influx (i.e. concentration
90 per year) from the same samples; because influx calculations are time dependent, we have only
91 retained concentration data for such sites to allow for future improvements to age models.
92 Influx can be easily computed using data available in the RPD. We extracted published
93 charcoal records that do not appear in any version of the GCD from public repositories,
94 specifically PANGAEA (<https://www.pangaea.de/>), NOAA National Centre for
95 Environmental Information (<https://www.ncdc.noaa.gov/data-access/paleoclimatology-data>),
96 the Neotoma Paleocology Database (<https://www.neotomadb.org/>), the European Pollen
97 Database (<http://www.europeanpollendatabase.net/index.php>) and the Arctic Data Centre
98 (<https://arcticdata.io/catalog/>). Additional charcoal data, dating information and metadata were
99 provided directly by the authors. All the records in the current version of the database are listed
100 in the Supplementary Information (SI Table 1).

101

102 ***2.2 Structure of the database***

103 The data are stored in a relational database (MySQL), which consists of 10 linked tables,
104 specifically "site", "entity", "sample", "date info", "unit", "entity link publication",
105 "publication", "chronology", "age model", and "model name". Figure 1 shows the relationships
106 between these tables. A description of the structure and content of each of the tables is given
107 below, and more detailed information about individual fields is given in the Supplementary
108 Material (SI Table 2).



109

110 *Figure 1. Entity-relation diagram showing the structure of the database, individual tables and*
 111 *their contents, and the nature of the relationships between the component tables. One-to-many*
 112 *linkages indicate that it is possible to have several entries on one table linked to a single entry*
 113 *in another table. The data base uses both primary and foreign keys. The primary key ensures*
 114 *that data included in a specific field is unique. The foreign key refers to the field in a table*
 115 *which is the primary key of another table and ensures that there is a link between these tables.*

116 **2.2.1 Site metadata (table name: site)**

117 A site is defined as the hydrological basin from which charcoal records have been obtained
 118 (Table 1). There may be several charcoal records from the same site, for example where
 119 charcoal records have been obtained on central and marginal cores from the same lake or where
 120 there is a lake core and additional cores from peatlands and/or terrestrial deposits (e.g. small
 121 hollows, soils) within the same hydrological basin. A site may therefore be linked to several
 122 charcoal records, where each record is treated as a separate entity. The site table contains basic
 123 metadata about the basin, including site ID, site name, latitude, longitude, elevation, site type,
 124 and maximum water depth. The site names are expressed without diacritics to facilitate
 125 database querying and subsequent analyses in programming languages that do not handle these
 126 characters. Latitude and longitude are given in decimal degrees, truncated to six decimal places
 127 since this gives an accuracy of <1m at the equator. Broad categories of site type are



128 differentiated (e.g. terrestrial, lacustrine, marine), with subdivisions according to geomorphic
 129 origin (e.g. lakes are recorded according to whether they are e.g. fluvial, glacial or volcanic in
 130 origin). In addition to coastal salt marshes and estuaries, we include a generic coastal category
 131 for all types of sites that lie within the coastal zone and the hydrology may therefore have been
 132 affected by changes in sea level. Wherever possible, the size of the basin and the catchment
 133 are recorded (in km²) but if accurate quantified information is not available the basin and
 134 catchment size are recorded by size classes. The site table also contains information on whether
 135 the lake or peatland is hydrologically closed or has inflows and outflows, which can affect the
 136 source, quantity and preservation of charcoal in the sediments.

137 Table 1 Definition of the site table.

Field name	Definition	Data type	Constraints / Notes
ID_SITE	Unique identifier for each site	Unsigned integer	positive integer
site_name	Site name as given by original authors or as defined by us where there was no unique name given to the site	Text	Required
latitude	Latitude of the sampling site, given in decimal degrees, where N is positive and S is negative	Double	Numeric value between -90 and 90
longitude	Longitude of the sampling site in decimal degrees, where E is positive and W is negative	Double	Numeric value between -180 and 180
elevation	Elevation of the sampling site in metres above (+) or below (-) sea level	Double	None
site_type	Information about type of site (e.g. lake, peatland, terrestrial)	Text	Selected from pre-defined list
water_depth	Water depth of the sampling site in metres	Double	None



flow_type	Indication of whether there is inflow and/or outflow from the sampled site	Text	Selected from pre-defined list
basin_size_km2	Size of sampled site (e.g. lake or bog) in km ²	Double	None
catch_size_km2	Size of hydrological catchment in km ²	Double	None
basin_size_class	Categorical estimate of basin size	Text	Selected from pre-defined list
catch_size_class	Categorical estimate of basin size	Text	Selected from pre-defined list

138

139 **2.2.2 Entity metadata (table name: entity)**

140 This table provides metadata for each individual entity (Table 2). In addition to distinguishing
 141 multiple cores from the same basin as separate entities, we also distinguish different size
 142 classes of charcoal from the same core when these data are available. Different charcoal size
 143 classes from the same core are also treated as separate entities in the database. When specific
 144 cores were given distinctive names in the original publication or by the original author, we
 145 include this information in the entity name for ease of cross-referencing. The entity metadata
 146 include information that can be used to interpret the charcoal records, including depositional
 147 context, core location, measurement method, and measurement unit. There is no standard
 148 measurement unit for charcoal, and in fact, there are >100 different units employed in the
 149 database. For convenience, there is a link table to the measurement units (table name: unit). In
 150 addition, the entity table provides the source from which the charcoal data were obtained,
 151 including whether these data are from a version of the GCD, a data repository or were provided
 152 by the original author, and an indication of when the record was last updated.

153 Table 2 Definition of the entity table.

Field name	Definition	Data type	Constraints / Notes
ID_ENTITY	Unique identifier for each entity	Unsigned integer	Positive integer



ID_SITE	Refers to unique identifier for each site (as given in site table)	Unsigned integer	Auto-numeric, foreign key of the site table, a positive integer
entity_name	Name of entity, where an entity may be a separate core from the site or a separate type of measurement on the same core	Text	Required
latitude	Latitude of the entity, given in decimal degrees, where N is positive and S is negative	Double	A numeric value between -90 and 90
longitude	Longitude of the entity, given in decimal degrees, where E is positive and W is negative	Double	A numeric value between -180 and 180
elevation	Elevation of the sampling site, in metres above (+) or below (-) sea level	Double	None
depositional_context	Type of sediment sampled for charcoal	Text	Selected from pre-defined list
measurement_method	Method used to measure the amount of charcoal	Text	Selected from pre-defined list
TYPE	The unit type of the measured charcoal values (e.g. concentration, influx)	Text	Selected from pre-defined list
source	Source of charcoal data	Text	Selected from pre-defined list
core_location	Location of the entity within the site (e.g. central core or marginal core)	Text	Selected from pre-defined list
last_updated	Date when the entity or its linked data was last updated	Date	In format YYYY/mm/dd



ID_UNIT	Unique identifier for measurement unit (as in unit table)	Unsigned integer	Auto-numeric, foreign key of the unit table, a positive integer
---------	---	------------------	---

154

155 **2.2.3 Sample metadata and data (table name: sample)**

156 The sample table provides information on the average depth in the core or profile and the
 157 thickness of the sample on which charcoal was measured. The thickness measurements relate
 158 to the total thickness of the charcoal sample and provide an indication of whether the sampling
 159 was contiguous downcore. The sample table also provides information on the sample volume
 160 and the quantity of charcoal present.

161 Table 3 Definition of the sample table.

Field name	Definition	Data type	Constraints / Notes
ID_SAMPLE	Unique identifier for each charcoal sample	Unsigned integer	Auto-numeric, primary key, a positive integer
ID_ENTITY	Unique identifier for the entity (as in entity table)	Unsigned integer	Auto-numeric, foreign key of the entity table, a positive integer
avg_depth	Average sampling depth, in metres	Double	None
sample_thickness	Sample thickness, in metres	Double	None
charcoal_measurement	Quantity of charcoal measured in the sample	Double	None
analytical_sample_volume	Total amount of sediment sampled	Text	255 characters maximum length

162



163 **2.2.4 Dating information (table name: date info)**

164 This table provides information about the dates available for each entity that can be used to
 165 construct an age model. We include information about the age of the core top for records that
 166 were known to be actively accumulating sediment at the time of collection. In addition to
 167 radiometric dates, we include information about the presence of tephras (either dated at the site
 168 or independently dated elsewhere) and stratigraphic events that can be used to establish
 169 correlative ages (e.g. changes in the pollen assemblage that are dated in other cores from the
 170 region, or evidence of known fires in the catchment). Wherever possible the name of a tephra
 171 is given, to facilitate the use of subsequent and more accurate estimates of its age. Similarly,
 172 the basis for correlative dates is given, again to facilitate the use of updated estimates of the
 173 age of the event. Radiocarbon ages are given in radiocarbon years, but all other ages are given
 174 in calendar years BP using 1950 CE as the reference zero date. Error estimates are given for
 175 radiometric ages and wherever possible for calendar ages. We provide an indication of whether
 176 a specific date was used in the original age model for the entity, and an explanation for why
 177 specific dates were rejected, since this can be a guide as to whether the dates should be
 178 incorporated in the construction of new age models.

179 Table 4 Definition of the date info table.

Field name	Definition	Data type	Constraints / Notes
ID_DATE_INFO	Unique identifier for the date record	Unsigned integer	Auto-numeric, primary key, a positive integer
ID_ENTITY	Unique identifier for the entity (as in entity table)	Unsigned integer	Auto-numeric, foreign key of the entity table, a positive integer
material_dated	Material from which the date was obtained, if applicable	Text	Selected from pre-defined list
date_type	Technique used to obtain the date measurement	Text	Selected from pre-defined list
avg_depth	Average depth in the sedimentary sequence	Double	None



	where the date was measured, in metres		
thickness	Thickness of the sample used for dating, in metres	Double	None
lab_number	Unique identifying code assigned by the dating laboratory	Text	65,535 characters maximum length
age_C14	Uncalibrated radiocarbon age	Double	None
age_calib	The calendar age of a date	Double	None
error	Analytical or measurement error on the date	Double	None
correlation_info	Indication of basis for correlative dating (e.g. pollen, tephra or stratigraphic correlations)	Text	Selected from pre-defined list
age_used	Indicates whether date was used by the author(s) in the construction of the original age model	Text	Selected from pre-defined list
reason_age_not_used	Indication of why a date was not used in the original age model. Blank if dates were used in original model	Text	Selected from pre-defined list
notes	Additional comments regarding a date record	Text	The maximum length is 65,535 characters

180

181 **2.2.5 Publication information (table name: publication)**

182 This table provides full bibliographic citations for the original references documenting the
 183 charcoal records and/or their age models. There may be multiple publications for a single



184 charcoal record, and all of these references are listed. Conversely, there may be a single
185 publication for multiple charcoal records. There is also a table (table name:
186 entity_link_publication) that links the publications to the specific entity.

187 **2.2.6 Original age model information (table name: chronology)**

188 This table provides information about the original age model for each record, and the ages
189 assigned to individual samples. There can be many records that use the same type of age model
190 (e.g. linear interpolation, spline, regression), and for convenience, there is a table that links the
191 records to the age model name (table name: model name).

192 **2.2.7 New age model information (table name: age_model)**

193 This table contains information about the age models that have been constructed for this version
194 of the database using the INTCAL2020 calibration curve (Reimer et al., 2020) and the BACON
195 (Blaauw et al., 2021) age modelling R package (see section 2.3). We preserve information on
196 the mean and median ages, as well as the quantile ranges for each sample.

197 Table 5 Definition of the age model table.

Field name	Definition	Data type	Constraints / Notes
ID_MODEL	Unique identifier for the technique used to generate the original age model	Unsigned integer	Auto-numeric, composite primary key with ID_SAMPLE, foreign key of the model_name table, positive integer
ID_SAMPLE	Unique identifier for the sample (as in sample table)	Unsigned integer	Auto-numeric, composite primary key with ID_MODEL, foreign key of the sample table, positive integer
mean	Mean age of the sample	Integer	None



median	Median age of the sample	Integer	None
UNCERT_5	Lower bound of the 95% confidence interval for the median age	Integer	None
UNCERT_95	Upper bound of the 95% confidence interval for the median age	Integer	None
UNCERT_25	Lower bound of the 75% confidence interval for the median age	Integer	None
UNCERT_75	Upper bound of the 75% confidence interval for the median age	Integer	None

198

199

200 **2.3 Construction of new age models**

201 The original age models for the charcoal records were made at different times, using different
202 radiocarbon calibration curves, and using different age-modelling methods. We standardised
203 the age modelling, using RBAcon (Blaauw and Christen, 2011; Blaauw et al., 2021) to construct
204 new Bayesian age-depth models in the ageR package (Villegas-Diaz et al., 2021). The ageR
205 package provides functions that facilitate the supervised creation of multiple age models for
206 many cores and different data sources, including databases, comma and tab separated files. The
207 INTCAL20 Northern Hemisphere calibration curve (Reimer et al., 2020) and the SHCAL20
208 Southern Hemisphere calibration curve (Hogg et al., 2020) were used for entities between the
209 latitudes of 90° and 15°N and 15 to 90°S respectively. Entities in equatorial latitudes (15°N to
210 15°S) used a 50:50 mixed calibration curve to account for north-south air mass-mixing
211 following Hogg et al. (2020), and radiocarbon ages from marine entities were calibrated using
212 the Marine20 calibration curve (Heaton et al., 2020).

213

214 To estimate the optimum age modelling scenarios based upon the date and sample information
215 for each entity, multiple RBAcon age models were run using different *prior* accumulation rate
216 (acc.mean) and thickness values. *Prior* accumulation rate values were selected using an initial



217 linear regression of the ages in each entity, which was then increased (decreased) sequentially
218 from the default value up to twice more (less) than the initial value. As an example, if the initial
219 accumulation rate value selected from the linear regression was 20 yr/cm, age models would
220 also be run using values of 10, 15, 20, 30 and 40 yr/cm. In cases where the regional
221 accumulation rate was known, the upper and lower values of the accumulation rate scenarios
222 were manually constrained. The range of *prior* thicknesses used in the models were calculated
223 by increasing and decreasing the R Bacon default thickness value (5 cm) up to a value one
224 eighth of the overall length of the core. For a 400 cm core for example, the thickness scenarios
225 would be 5, 10, 15, 20, 25, 30, 35, 40, 45 and 50 cm. Thus, the number of scenarios created by
226 possible accumulation rates and thicknesses varies between different entities. Depths of known
227 hiatuses reported in the original publications were included in the date info table (section 2.2.4)
228 and have also been included in the age models run in ageR. In instances where the
229 sedimentation rates were different above and below an hiatus, separate age models were run
230 before and after the non-deposition period to account for these variations (Blaauw and Christen,
231 2011).

232

233 A three-step procedure was used to select the best model for each entity. First, an optimum
234 model was selected by ageR, using the lowest quantified area between the *prior* and *posterior*
235 accumulation rate distribution curves (Supplementary Figure 1). This selection was checked
236 manually using comparisons between the distance of the estimated ages and the controls to
237 check the accuracy of the model interpolation. Finally, the age model was visually inspected
238 to ensure that final interpolation accurately represented the date information and did not show
239 abrupt shifts in accumulation rates or changes at the dated depths. If the ageR model selection
240 was deemed to be erroneous or inaccurate, the next suitable model with the lowest area between
241 the *prior* and *posterior* curves, which accurately represented the distribution of dates in the
242 sequence, was selected (Supplementary Figure 2).

243

244 **2.4 Quality control**

245 Individual records in the RPD were compiled either by the original authors or from published
246 and open-access material by specialists in the collection and interpretation of charcoal records.
247 Records that were obtained from published and open-access material were cross-checked
248 against publications or with the original authors of those publications whenever possible. Null
249 values for metadata fields were identified during the initial checking procedure, and checks



250 were made with the data contributors to determine whether these genuinely corresponded to
251 missing information. In the database, null values are reserved for fields where the required
252 information is not applicable, for example water depth for terrestrial sites or laboratory sample
253 numbers for correlative dates. We distinguish fields where information could be available but
254 was never recorded or has subsequently been lost (represented by -999999), and fields where
255 we were unable to obtain this information but it could be included in subsequent updates of the
256 database (represented by -777777). We also distinguish fields where specific metadata is not
257 applicable (represented by -888888), for example basin size for a marine core or water depth
258 for a terrestrial small hollow.

259 Prior to entry in the database, the records were automatically checked using specially designed
260 database scripts (in R) to ensure that the entries to individual fields were in the format expected
261 (e.g. text, decimal numeric, positive integers) or were selected from the pre-defined lists
262 provided for specific fields. Checks were also performed to find duplicated rows (e.g.
263 duplicated sampling depths within the same entity).

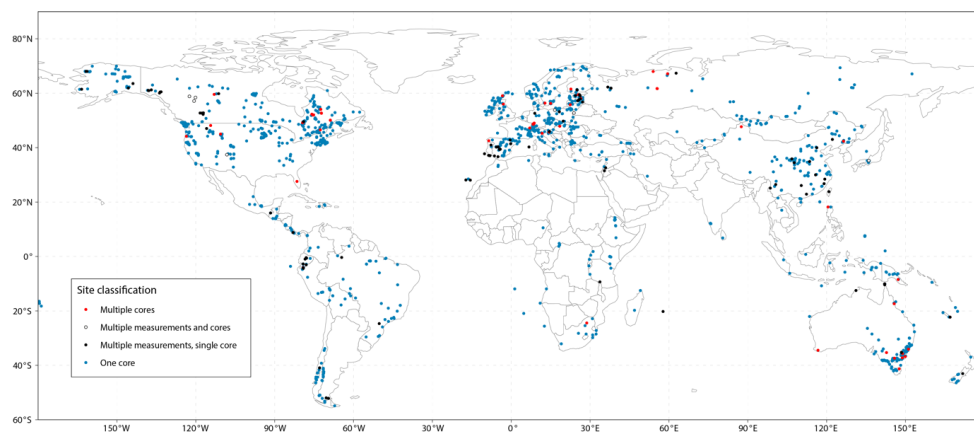
264

265 **3. Overview of database contents**

266 This first version of the RPD contains 1681 individual charcoal records from 1477 sites
267 worldwide. This represents a 101% increase compared to the number of records in version 3
268 of the Global Charcoal Database (GCDv3: Marlon et al., 2016; 736 sites) and a 58% increase
269 compared to version 4 (Blarquez, 2018; 935 sites). New age models are available for 714 (48%)
270 of the charcoal records. The geographic coverage of the RPD (Figure 2) is biased towards the
271 northern extratropics. However, there is a growing representation of records from China, the
272 Neotropics (Central and South America), southern and eastern Africa, and eastern Australia.
273 The largest gaps geographically are in currently dry regions, which often lack sites with anoxic
274 sedimentation suitable for the preservation of charcoal and are generally under-represented in
275 palaeofire reconstructions (Leys et al., 2018). The temporal coverage of the records is excellent
276 for the interval since 22,000 years ago, with 776 records with a minimum resolution of 10 years
277 for the past 2000 years, 1338 records with a minimum resolution of 500 years for the past
278 12,000 years, and 1385 records with a minimum resolution of 1000 years for the past 22,000
279 years. There are fewer records for earlier intervals. Nevertheless, there are 70 records that
280 provide evidence for the interval of the last glacial period before the Last Glacial Maximum



281 (22-115 ka) including the response of fire to rapid climate warmings (Dansgaard-Oeschger
282 events).

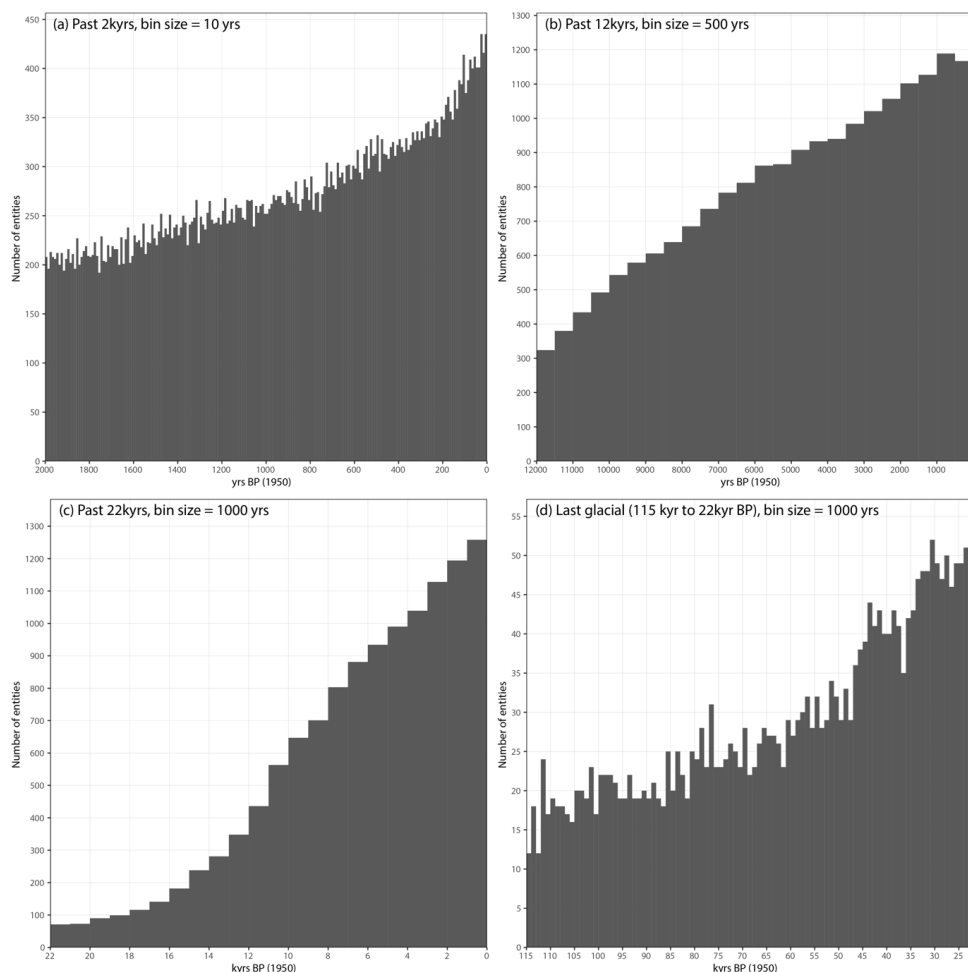


283

284 *Figure 2. Map showing the location of sites included in the RPD. As shown here, some sites*
285 *have multiple records, either representing separate cores from the same hydrological basin or*
286 *representing measurements of different charcoal size fractions on the same core. These records*
287 *are treated as separate entities in the database itself.*

288

289



290

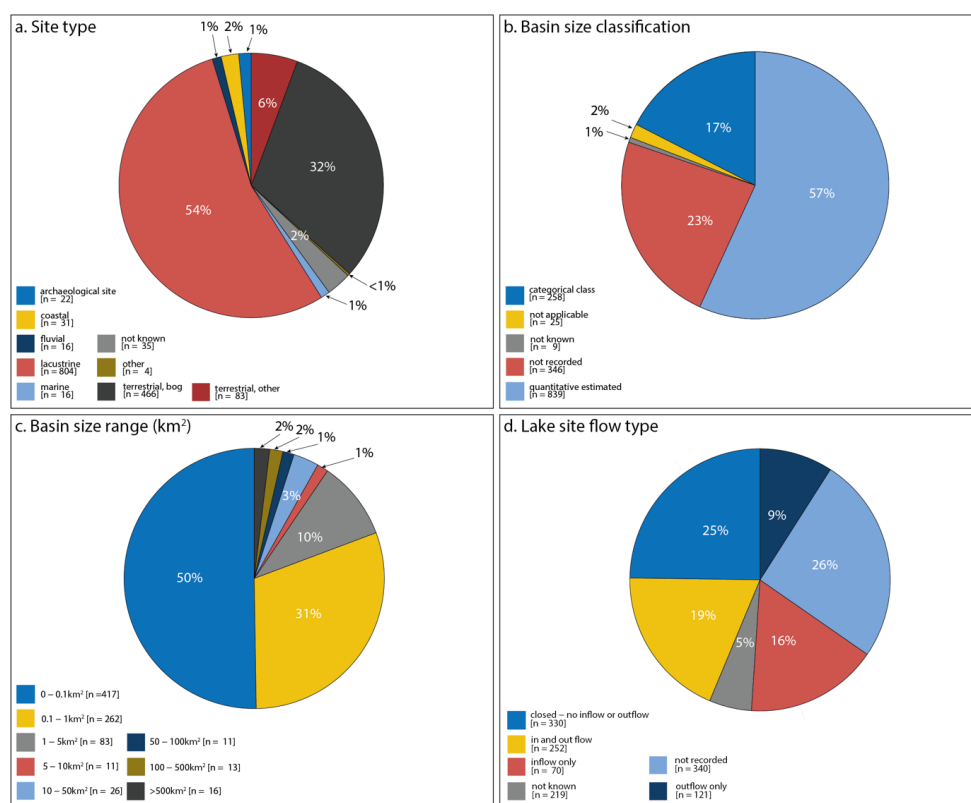
291 *Figure 3. Plot showing the temporal coverage of individual entities in the database. Panel (a)*
292 *shows records covering the past 2000 years (2kyrBP), (b) shows records covering the past*
293 *12,000 years, (c) for the past 22 000 years (22 kyr BP) and thus encompassing the Last Glacial*
294 *Maximum (LGM), and (d) shows records that cover the interval of the last glacial prior to the*
295 *LGM (22–115 kyr BP).*

296

297 Information about site type (Figure 4a) is included in the database because this could influence
298 whether the charcoal is of local origin or represents a more regional palaeofire signal. For
299 example, records from small forest hollows provide a very local signal of fire activity and
300 records from peatbogs most likely sample fires on the peatland itself, whereas records from
301 lakes could provide both local and regional fire signals. More than half (54%) of the records in
302 the RPD are derived from lakes (804 entities). Records from peatlands are also well represented



303 (466 entities, 32%). Basin size, particularly in the case of lakes, influences the source area for
 304 charcoal particles transported by wind. However, the existence of inflows and outflows to the
 305 system can also affect the charcoal record. Quantitative information is now available for more
 306 than half of the lake sites (Figure 4b), and most (679 sites, 81%) of the records (Figure 4c) are
 307 from relatively small lakes (<1 km²). A quarter of the charcoal records from lakes (Figure 4d)
 308 are from closed basins (330 sites).



309
 310 *Figure 4. Availability of metadata that can be used to select suitable sites for specific analyses*
 311 *or for quality control. Plot (a) shows the distribution of sites by type. Some site types have finer*
 312 *distinctions recorded in the database: lacustrine environments, for example, are sub-divided*
 313 *according to origin. Plot (b) shows the number of sites with quantitative estimates versus*
 314 *categorical assessments of basin size and plot (c) shows the number of sites in specific basin*
 315 *size ranges. Plot (d) shows the distribution of different hydrological types for lake records.*
 316

317 4. Data availability

318

319 Version 1 of the Reading Palaeofire Database (RPDv1: Harrison et al., 2021, doi:
 320 10.17864/1947.319) is available in SQL format from



321 <https://researchdata.reading.ac.uk/id/eprint/319>. The R package used to create the new age
322 models is available from <https://github.com/special-uor/ageR> (Villegas-Diaz et al., 2021).

323

324

325 **5. Conclusions**

326 The Reading Palaeofire Database (RPD) is a community effort to improve the coverage of
327 charcoal records that can be used to investigate palaeofire regimes. New age models have been
328 developed for 48% of the records to take account of recent improvements in radiocarbon
329 calibration and age modelling methods. In addition to expanded coverage and improved age
330 models, considerable effort has been made to include metadata and quality control information
331 to allow the selection of records appropriate to address specific questions and to document
332 potential sources of uncertainty in the interpretation of the records. The first version of the RPD
333 contains 1681 individual charcoal records (entities) from 1477 sites worldwide. Geographic
334 coverage is best for the northern extratropics, but the coverage is good except for semi-arid and
335 arid regions. Temporal coverage is good for the past 2000 years, the Holocene and back to the
336 LGM, but there is a reasonable number of longer records. The database is publicly available.

337

338

339

340 **Author contributions.** SPH and RV-D designed the data base; RV-D, DK, PL and SPH were
341 responsible for construction of the database; A-LD advised on incorporation of data from the
342 GCD and the standardisation of charcoal units; EC-S, DG, DK, PL, YS, LS provided updated
343 age models; the other authors provided original data or metadata and quality control on
344 individual records; SPH wrote the first draft of the paper and all authors contributed to the final
345 draft.

346

347 **Competing Interests.** The authors declare that they have no conflict of interest.

348

349 **Acknowledgements.** RV-D, SPH, EC-S, and YS acknowledge support from the ERC-funded
350 project GC2.0 (Global Change 2.0: Unlocking the past for a clearer future, grant number
351 694481). SPH, PL, DG, DK, LS acknowledge support from the Leverhulme Centre for
352 Wildfires, Environment and Society through the Leverhulme Trust, grant number RC-2018-
353 023. AF acknowledges support from the German Research Foundation (grant no. FE-1096/6-
354 1). KM acknowledges support from the Swiss Government Excellence Postdoctoral



355 Scholarship (grant no. FIRECO 2016.0310); the National Science Centre in Poland (grant no.
356 2015/17/B/ST10/01656); grant PSPB-013/2010 from Switzerland through the Swiss
357 Contribution to the enlarged European Union; the Scientific Exchange Programme from the
358 Swiss Contribution to the New Member States of the European Union (Sciex-NMS ch) –
359 SCIEX Scholarship Fund, project RE-FIRE 12.286. OL acknowledges support from the
360 Mobilitas Plus post-doctoral research grant of The Estonian Research Council (MOBJD313).
361 We would like to thank our many colleagues from the PAGES Global Palaeofire Working
362 Group for their contributions to the construction of the Global Charcoal Database which
363 provided the starting point for the current compilation, and our colleagues from the Leverhulme
364 Centre for Wildfires, Environment and Society for discussions of the use of palaeodata to
365 reconstruct past fire regimes. We thank Manfred Rösch for providing information on dating
366 for several sites.
367



368 **References**

- 369 Arora, V. K. and Melton, J. R.: Reduction in global area burned and wildfire emissions since
370 1930s enhances carbon uptake by land, *Nat. Commun.*, 9, 1326,
371 <https://doi.org/10.1038/s41467-018-03838-0>, 2018.
- 372 Bistinas, I., Harrison, S. P., Prentice, I. C., and Pereira, J. M. C.: Causal relationships vs.
373 emergent patterns in the global controls of fire frequency, *Biogeosci.*, 11, 5087-5101,
374 2014.
- 375 Blaauw, M.J. Christen, A.: Flexible paleoclimate age-depth models using an autoregressive
376 gamma process, *Bayesian Analysis*, 6, 457-474, <https://doi.org/10.1214/11-BA618>,
377 2011.
- 378 Blaauw, M., Christen, J.A., Aquino Lopez, M.A., Esquivel Vazquez, J., Gonzalez, O.M.,
379 Belding, T., Theiler, J., Gough, B., Karney, C.: rbacon: Age-Depth Modelling using
380 Bayesian Statistics, <https://CRAN.R-project.org/package=rbacon>, 2021.
- 381 Blarquez, O.: GCD, <https://CRAN.R-project.org/package=GCD>, 2018.
- 382 Blarquez, O., Vanni re, B., Marlon, J. R., Daniau, A-L., Power, M. J., Brewer, S. and Bartlein,
383 P. J. paleofire: An R package to analyse sedimentary charcoal records from the Global
384 Charcoal Database to reconstruct past biomass burning, *Computers & Geosci.*, 72, 255-
385 261, <https://doi.org/10.1016/j.cageo.2014.07.020>, 2014.
- 386 Bond, W. J., Woodward, F. I., and Midgley, G. F.: The global distribution of ecosystems in a
387 world without fire, *New Phytol.*, 165, 525–538, 2005.
- 388 Bowman, D. M. J. S., Perry, G. L. W., Higgins, S. I., Johnson, C. N., Fuhlendorf, S. D., and
389 Murphy, B. P.: Pyro- diversity is the coupling of biodiversity and fire regimes in food
390 webs, *Philos. T. R. Soc. Lond.*, 371, 20150169, <https://doi.org/10.1098/rstb.2015.0169>,
391 2016.
- 392 Daniau, A.-L., Bartlein, P. J., Harrison, S. P., Prentice, I. C., Brewer, S., Friedlingstein, P.,
393 Harrison-Prentice, T. I., Inoue, J., Marlon, J. R., Mooney, S., Power, M. J., Stevenson,
394 J., Tinner, W., Andri , M., Atanassova, J., Behling, H., Black, M., Blarquez, O., Brown,
395 K. J., Carcaillet, C., Colhoun, E., Colombaroli, D., Davis, B. A. S., D’Costa, D.,
396 Dodson, J., Dupont, L., Eshetu, Z., Gavin, D. G., Genries, A., Gebru, T., Haberle, S.,
397 Hallett, D. J., Horn, S., Hope, G., Katamura, F., Kennedy, L., Kershaw, P., Krivonogov,
398 S., Long, C., Magri, D., Marinova, E., McKenzie, G. M., Moreno, P. I., Moss, P.,
399 Neumann, F. H., Norstr m, E., Paitre, C., Rius, D., Roberts, N., Robinson, G., Sasaki,
400 N., Scott, L., Takahara, H., Terwilliger, V., Thevenon, F., Turner, R. B., Valsecchi, V.
401 G., Vanni re, B., Walsh, M., Williams, N., and Zhang, Y.: Predictability of biomass



- 402 burning in response to climate changes, *Glob. Biogeochem. Cyc.*, 26, GB4007,
403 doi:10.1029/2011GB004249, 2012.
- 404 Daniau, A.-L., Harrison S. P. and Bartlein, P. J.: Fire regimes during the last glacial, *Quat. Sci.*
405 *Rev.*, 29: 2918-2930, 2010.
- 406 Forkel, M., Dorigo, W., Lasslop, G., Teubner, I., Chuvieco, E., and Thonicke, K.: A data-
407 driven approach to identify controls on global fire activity from satellite and climate
408 observations (SOFIA V1), *Geosci. Model Dev.*, 10, 4443–4476,
409 <https://doi.org/10.5194/gmd-10-4443-2017>, 2017.
- 410 Feurdean, A., Vannière, B., Finsinger, W., Warren, D., Connor, S. C., Forrest, M., Liakka, J.,
411 Panait, A., Werner, C., Andrič, M., Bobek, P., Carter, V. A., Davis, B., Diaconu, A.-
412 C., Dietze, E., Feeser, I., Florescu, G., Gařka, M., Giesecke, T., Jahns, S., Jamrichová,
413 E., Kajukařo, K., Kaplan, J., Karpińska-Kořaczek, M., Kořaczek, P., Kuneř, P.,
414 Kupriyanov, D., Lamentowicz, M., Lemmen, C., Magyari, E. K., Marcisz, K.,
415 Marinova, E., Niamir, A., Novenko, E., Obremska, M., Pędziszewska, A., Pfeiffer, M.,
416 Poska, A., Rōsch, M., Słowiński, M., Stančikaitė, M., Szal, M., Święta-Musznicka, J.,
417 Tanřau, I., Theuerkauf, M., Tonkov, S., Valkó, O., Vassiljev, J., Veski, S., Vincze, I.,
418 Wacnik, A., Wiethold, J., Hickler, T.: Fire hazard modulation by long-term dynamics
419 in land cover and dominant forest type in eastern and central Europe, *Biogeosci.*, 17,
420 1213-1230, 10.5194/bg-17-1213-2020, 2020.
- 421 Harrison, S. P., Bartlein, P. J., Brovkin, V., Houweling, S., Kloster, S., and Prentice, I. C.:
422 Biomass burning contribution to global climate-carbon cycle feedback, *Earth System*
423 *Dyn.*, 9, 663-67, <https://doi.org/10.5194/esd-9-663-2018>, 2018.
- 424 Harrison, S. P., Marlon, J. R., Bartlein, P. J.: Fire in the Earth System, In *Changing Climates,*
425 *Earth Systems and Society International Year of Planet Earth*, pp 21-48. Springer
426 Publisher, 2010.
- 427 Harrison, S.P, Villegas-Diaz, R., Lincoln, P., Kesner, D., Cruz-Silva, E., Sweeney, L., Shen,
428 Y. and Gallagher, D.: The Reading Palaeofire Database: an expanded global resource
429 to document changes in fire regimes from sedimentary charcoal records. University of
430 Reading Dataset. <http://dx.doi.org/10.17864/1947.319>;
431 <https://researchdata.reading.ac.uk/id/eprint/319>, 2021
- 432 He, T., Lamont, B. B., and Pausas, J. G.: Fire as a key driver of Earth's biodiversity, *Biol. Rev.*,
433 94, 1983–2010, <https://doi.org/10.1111/brv.12544>, 2019.
- 434 Heaton, T., Köhler, P., Butzin, M., Bard, E., Reimer, R., Austin, W., Bronk Ramsey, C.,
435 Grootes, P. M., Highen, K. A., Kromer, B., Reimer, P. J., Adkins, A., Burke, A. M.,



- 436 Cook, M. S., Olsen, J., and Skinner, L.: Marine 20 — The marine radiocarbon age
437 calibration curve (0-55,000 cal BP), *Radiocarbon*, 62, 779-820, doi:
438 10.1017/RDC.2020.68, 2020.
- 439 Hogg, A., Heaton, T., Hua, Q., Palmer, J., Turney, C., Southon, J., Bayliss, A., Blackwell, P.
440 G., Boswijk, G., Bronk Ramsey, C., Pearson, C., Petchey, F., Reimer, P., Reimer, R.,
441 and Wacker, L.: SHCal 20 southern Hemisphere calibration, 0-55,000 years cal BP,
442 *Radiocarbon*, 62, 759-778, doi: 10.1017/RDC.2020.59, 2020.
- 443 Knorr, K., Jiang, L. and Arneth, A.: Climate, CO₂, and demographic impacts on global wildfire
444 emissions, *Biogeosci.*, 12, 267-282, 10.5194/bgd-12-15011-2015, 2016.
- 445 Lasslop, G., Coppola, A. I., Voulgarakis, A., Yue, C., and Veraverbeke, S.: Influence of fire
446 on the carbon cycle and climate, *Current Clim. Change Rep.*, 5, 112–123,
447 <https://doi.org/10.1007/s40641-019-00128-9>, 2019.
- 448 Lasslop, G., Hantson, S., Harrison, S. P., Bachelet, D., Burton, C., Forkel, M., Forrest, M., Li,
449 F., Melton, J. R., Yue, C., Archibald, S., Scheiter, S., Arneth, A., Hickler, T., and Sitch,
450 S.: Global ecosystems and fire: multi-model assessment of fire-induced tree cover and
451 carbon storage reduction, *Glob. Change Biol.*, 26, 5027-5041, 10.1111/gcb.15160,
452 2020.
- 453 Leys, B., Marlon, J.R., Umbanhowar, C., Vanniene, B. (2018). Global fire history of grassland
454 biomes. *Ecology and Evolution* 8 (17), 8831-8852.
- 455 Li, F., Bond-Lamberty, B., Levis, S., 2014. Quantifying the role of fire in the Earth system—
456 Part 2: Impact on the net carbon balance of global terrestrial ecosystems for the 20th
457 century. *Biogeosciences* 11, 1345–1360.
- 458 Li, F., Lawrence, D. M. and Bond-Lamberty, B.: Impact of fire on global land surface air
459 temperature and energy budget for the 20th century due to changes within
460 ecosystems, *Environ. Res. Lett.*, 12, 044014, 2017.
- 461 Li, F., Val Martin, M., Andreae, M. O., Arneth, A., Hantson, S., Kaiser, J. W., Lasslop, G.,
462 Yue, C., Bachelet, D., Forrest, M., Kluzek, E., Liu, X., Mangeon, S., Melton, J. R.,
463 Ward, D. S., Darnenov, A., Hickler, T., Ichoku, C., Magi, B. I., Sitch, S., van der Werf,
464 G. R., Wiedinmyer, C., and Rabin, S. S.: Historical (1700–2012) global multi-model
465 estimates of the fire emissions from the Fire Modeling Intercomparison Project
466 (FireMIP), *Atmos. Chem. Phys.*, 19, 12545–12567, <https://doi.org/10.5194/acp-19-12545-2019>, 2019.
- 467



- 468 Liu, Z., Ballantyne, A. P. and Cooper, L. A.: Biophysical feedback of global forest fires on
469 surface temperature, *Nat. Commun.*, 10, 214, [https://doi.org/10.1038/s41467-018-](https://doi.org/10.1038/s41467-018-08237-z)
470 08237-z, 2019.
- 471 Marlon, J., Bartlein, P. J., Carcaillet, C., Gavin, D. G., Harrison, S. P., Higuera, P. E., Joos, F.,
472 Power, M., and Prentice, I. C.: Climate and human influences on global biomass
473 burning over the past two millennia, *Nature Geosci.*, 1, 697-702, doi: 10.1038/ngeo313,
474 2008.
- 475 Marlon, J.R., Bartlein, P. J., Daniau, A.-L., Harrison, S. P., Power, M. J., Tinner, W.,
476 Maezumie, S., and Vannière, B.: Global biomass burning: A synthesis and review of
477 Holocene paleofire records and their controls, *Quat. Sc. Rev.*, 65, 5-25, 2013.
- 478 Marlon, J.R., Bartlein, P. J., Long, C., Gavin, D. G., Anderson, R. S., Briles, C., Brown, K.,
479 Colombaroli, D., Hallett, D. J., Power, M. J., Scharf, E., and Walsh, M. K.: Long-term
480 perspective on wildfires in the western U.S.A. *Proc. Nat. Acad. Sci.*, 109, E535-
481 E543, <https://doi.org/10.1073/pnas.1112839109>, 2012.
- 482 Marlon, J. R., Bartlein, P. J., Walsh, M. K., Harrison, S. P., Brown, K. J., Edwards, M. E.,
483 Higuera, P. E., Power, M. J., Anderson, R. S., Briles, C., Brunelle, A., Carcaillet, C.,
484 Daniels, M., Hu, F. S., Lavoie, M., Long, C., Minckley, T., Richard, P. J. H., Scott, A.
485 C., Shafer, D. S., Tinner, W., Umbanhowar, C. E. Jr., and Whitlock, C.: Wildfire
486 responses to abrupt climate change in North America. *Proc. Nat. Acad. Sci.*, 106, 2519-
487 2524, doi: 0.1073/pnas.0808212106, 2009.
- 488 Marlon, J., Bartlein, P. J., and Whitlock, C.: Fire-fuel-climate linkages in the northwestern
489 USA during the Holocene, *Holocene*, 16, 1059–1071, 2006.
- 490 Marlon, J. R., Kelly, R., Daniau, A.-L., Vannière, B., Power, M. J., Bartlein, P. J., Higuera,
491 P., Blarquez, O., Brewer, S., Brücher, T., Feurdean, A., Romera, G. G., Iglesias, V.,
492 Maezumi, S. Y., Magi, B., Courtney Mustaphi, C. J., and Zhihai, T.: Reconstructions
493 of biomass burning from sediment charcoal records to improve data-model
494 comparisons, *Biogeosci.*, 13, 3325–3244, doi:10.5194/bg-13-3225-2016, 2016.
- 495 Mooney, S., Harrison, S. P., Bartlein, P. J., Daniau A.-L., Stevenson, J., Brownlie, K.,
496 Buckman, S., Cupper, M., Luly, J., Black, M., Colhoun, E., D’Costa, D., Dodson, J.,
497 Haberle, S., Hope, G. S., Kershaw, P., Kenyon, C., McKenzie, M., Williams, N.: Late
498 Quaternary fire regimes of Australasia, *Quat. Sci. Rev.*, 30, 28-46, 2011.
- 499 Pellegrini, A. F. A., Ahlström, A., Hobbie, S. E., Reich, P. B., Nieradzik, L. P., Staver, A.
500 C., Scharenbroch, B. C., Jumpponen, A., William R. L. Anderegg, W. R. L., James T.
501 Randerson, J. T., and Jackson, R. B.: Fire frequency drives decadal changes in soil



- 502 carbon and nitrogen and ecosystem productivity, *Nature*, 553, 194–198.
503 <https://doi.org/10.1038/nature24668>, 2018.
- 504 Power, M. J., Mayle, F. E., Bartlein, P. J., Marlon, J. R., Anderson, R. S., Behling, H., Brown,
505 K. J., Carcaillet, C., Colombaroli, D., Gavin, D. G., Hallett, D. J., Horn, S. P., Kennedy,
506 L. M., Lane, C. S., Long, C. J., Moreno, P. I., Paitre, C., Robinson, G., Taylor, Z., and
507 Walsh, M. K.: 16th Century burning decline in the Americas: population collapse or
508 climate change? *Holocene*, 1-11, 2013.
- 509 Power, M. J., Marlon, J. R., Bartlein, P. J., and Harrison, S. P.: Fire history and the Global
510 Charcoal Database: a new tool for hypothesis testing and data exploration, *Palaeogeog.*,
511 *Palaeoclim.*, *Palaeoecol.*, 291, 52-59. doi: 10.1016/j.palaeo.2009.09.014, 2010.
- 512 Power, M. J., Ortiz, N., Marlon, J., Bartlein, P. J., Harrison, S. P., Mayle, F., Ballouche, A.,
513 Bradshaw, R., Carcaillet, C., Cordova, C., Mooney, S., Moreno, P., Prentice, I. C.,
514 Thonicke, K., Tinner, W., Whitlock, C., Zhang, Y., Zhao, Y., Anderson, R. S., Beer,
515 R., Behling, H., Briles, C., Brown, K., Brunelle A., Bush, M., Clark, J., Colombaroli,
516 D., Chu, C. Q., Daniels, M., Dodson, J., Edwards, M. E., Fisinger, W., Gavin, D. G.,
517 Gobet, E., Hallett, D. J., Higuera, P., Horn, S., Inoue, J., Kaltenrieder, P., Kennedy, L.,
518 Kong, Z. C., Long, C., Lynch, J., Lynch, B., McGlone, M., Meeks, S., Meyer, G.,
519 Minckley, T., Mohr, J., Noti, R., Pierce, J., Richard, P., Shuman, B. J., Takahara, H.,
520 Toney, J., Turney, C., Umbanhower, C., Vandergoes, M., Vanniere, B., Vescovi, E.,
521 Walsh, M., Wang, X., Williams, N., Wilmshurst, J., Zhang, J. H.: Changes in fire
522 activity since the LGM: an assessment based on a global synthesis and analysis of
523 charcoal data, *Clim. Dyn.*, 30: 887-907, doi: 10.1007/s00382.00.0334x, 2008.
- 524 Power, M. J., Whitlock, C., Bartlein, P. J., and Stevens, L.R.: Fire and vegetation history during
525 the last 3800 years in northwestern Montana, *Geomorph.*, 75, 420–436, 2006.
- 526 Power, M., Mayle, F., Bartlein, P., Marlon, J.R., Anderson, R.S., Behling, H., Brown, K.J.
527 Carcailler, C., Colombaroli, D., Gavin, D.G., Hallett, D.J., Horn, S.P., Kennedy, L.M.,
528 Lane, C.S., Long, C.J., Moreno, P.I., Paitre, C., Robinson, G., Taylor, Z., Walsh, M.K.:
529 Climatic control of the biomass-burning decline in the Americas after ad 1500. *The*
530 *Holocene*, 23, 3-13, doi:10.1177/0959683612450196, 2013.
- 531 Randerson, J. T., Liu, H., Flanner, M. G., Chambers, S. D., Jin, Y., Hess, P. G., Pfister, G.,
532 Mack, M. C., Treseder, K. K., Welp, L. R., Chapin, F. S., Hardeb, J. W., Goulden, M.L.
533 Lyons, E., Neff, J. C., Schuur, E. A. G., and Zender, C. S.: The impact of boreal forest
534 fire on climate warming, *Science*, 314, 1130–1132, 2006.



- 535 Reimer, P., Austin, W., Bard, E., Bayliss, A., Blackwell, P., Bronk Ramsey, C., Butzin, M.,
536 Cheng, H. Edwards, R.L., Friedrich, M., Grootes, P.M., Guilderson, T.P., Hajdas, I.,
537 Heaton, T.J., Hogg, A.G., Hughen, K.A., Kromer, B., Manning, S.W., Muscheler, R.,
538 Palmer, J.G., Pearson, C., van der Plicht, J., Reimer, R.W., Richards, D.A., Scott, E.M.,
539 Southon, J.R., Turney, C.S.M., Wacker, L., Adolphi, F., Buntgen, U., Capano, M.,
540 Fahrni, S.M., Fogtmann-Schulz, A., Friedrich, R., Kohler, P. Kudsk, S., Miyake, F.,
541 Olsen, J., Reinig, F., Sakamoto, M., Sookdeo, M., Talamo, S.: The INTCAL20
542 Northern Hemisphere radiocarbon age calibration curve (0-55 calkBP), *Radiocarbon*,
543 62, 725-757, doi: 10.1017/RDC.2020.21, 2020.
- 544 Rubino, M., D’Onofrio, A., Seki, O., and Bendle, J. A.: Ice- core records of biomass burning,
545 *Anthrop. Rev.*, 3, 140–162, <https://doi.org/10.1177/2053019615605117>, 2016.
- 546 Sokolik, I. N., Soja, A. J., DeMott, P. J., and Winker, D.: Progress and challenges in
547 quantifying wildfire smoke emissions, their properties, transport, and atmospheric
548 impacts. *J. Geophys. Res: Atmos.*, 124, 13005-12025,
549 <https://doi.org/10.1029/2018JD029878>, 2019.
- 550 van der Werf, G. R., Randerson, J. T., Giglio, L., Collatz, G. J., Mu, M., Kasibhatla, P. S.,
551 Morton, D. C., DeFries, R. S. Jin, Y., and van Leeuwen, T. T.: Global fire emissions
552 and the contribution of deforestation, savanna, forest, agricultural, and peat fires (1997–
553 2009). *Atmos. Chem. Physics*, 10, 11707–11735. [https://doi.org/10.5194/acp-10-](https://doi.org/10.5194/acp-10-11707-2010)
554 [11707-2010](https://doi.org/10.5194/acp-10-11707-2010), 2010.
- 555 Vanni re, B., Power, M. J., Roberts, N., Tinner, W., Carri n, J., Magny, M., Bartlein, P. J., and
556 GPWG contributors: Circum-Mediterranean fire activity and climate changes during
557 the mid Holocene environmental transition (8500-2500 cal yr BP), *Holocene*, 21, 53-
558 73, 2011.
- 559 Villegas-Diaz, R., Cruz-Silva, E., Harrison, S. P. ageR: Supervised Age Models.
560 doi:10.5281/zenodo.4636716, 2021.
- 561 Voulgarakis, A., and Field, R. D. Fire influences on atmospheric composition, air quality and
562 climate, *Curr. Pollution Rep.*, 1, 70–81, <https://doi.org/10.1007/s40726-015-0007-z>,
563 2015.
- 564 Williams, A. N., Mooney, S. D., Sisson, S. A., and Marlon, J. R.: Exploring the relationship
565 between Aboriginal population indices and fire in Australia over the last 20,000 years,
566 *Palaeogeog., Palaeoclim., Palaeoecol.*, 432, 49-57, 2015.